frontiers | Frontiers in Astronomy and Space Sciences

TYPE Original Research
PUBLISHED 30 August 2024
DOI 10.3389/fspas.2024.1452513

OPEN ACCESS

EDITED BY
Shiwei Feng,
Shandong University, Weihai, China

REVIEWED BY
Alexander Nindos,
University of Ioannina, Greece
Peijin Zhang,
University of Helsinki, Finland

*CORRESPONDENCE
Jingye Yan,
yanjingye@nssc.ac.cn

RECEIVED 21 June 2024
ACCEPTED 13 August 2024
PUBLISHED 30 August 2024

CITATION
Yan J and Yu Q (2024) Statistical geoeffectiveness of solar-interplanetary disturbance events of type II radio bursts and CMEs/shocks.
Front. Astron. Space Sci. 11:1452513.
doi: 10.3389/fspas.2024.1452513

Statistical geoeffectiveness of solar-interplanetary disturbance events of type II radio bursts and CMEs/shocks

Jingye Yan[1,2]* and Quanyingqi Yu[1,3]

[1]State Key Laboratory of Space Weather, National Space Science Center, Chinese Academy of Sciences, Beijing, China, [2]Radio Science and Technology Center (πCenter), Chengdu, China, [3]University of Chinese Academy of Sciences, Beijing, China

Understanding and predicting the geoeffectiveness of solar activity on Earth is crucial for space weather. Therefore, predicting the impact of coronal mass ejections (CMEs) and their associated interplanetary (IP) shocks on Earth is essential. Observations of CMEs near the Sun can be used for these prediction and to study their propagation and evolution in IP space. Commonly used international models do not accurately predict whether and when IP shocks would reach Earth, thus failing to meet the demands of space weather forecasting. This study investigated the geoeffectiveness of solar-IP disturbance events, focusing on type II radio bursts from 1996 to 2019 (solar cycles 23 and 24). The study results showed that during this period, Wind/WAVES detected 623 type II bursts and 541 IP shocks at the L1 point, where 181 type II bursts were associated with L1 shocks. Approximately 29% of the IP shocks associated with type II bursts reached Earth, and approximately 34% of the IP shocks at the L1 point were accompanied by these bursts. IP type II radio bursts and their cutoff frequencies can serve as indicators of the geoeffectiveness of CMEs towards Earth. IP shocks accompanied by type II radio bursts cause stronger geomagnetic responses than those without the associated type II radio bursts. Lower cutoff frequencies of type II radio bursts increase the probability that the corresponding shocks reaching Earth, intensifying the geomagnetic response of the shock. Consequently, the presence of IP type II radio bursts and can serve as indicators of geoeffectiveness of the Earth-directed CMEs. Further, they help improve the accuracy of forecasting the geoeffectiveness of CME/shock events towards Earth.

KEYWORDS

type II radio bursts, shock, coronal mass ejection, geomagnetic storm, geoeffectiveness

1 Introduction

A CME is a phenomenon in which large-scale magnetized plasma is ejected from the solar atmosphere into IP space (Hundhausen, 1987; Gopalswamy et al., 2008a). Additionally, it is a crucial activity in the solar atmosphere and system, closely associated with space weather. It erupts from the closed magnetic field regions on the sun and propagates through the ambient medium. The CME propagates through the solar corona and IP space, generating IP shocks when their velocity exceeds

the Alfven speed in the background solar wind. When these IP shocks traverse the surrounding medium, they excite nonthermal electrons, enhancing electromagnetic radiation at frequencies close to the local plasma frequency. This enhancement in electromagnetic radiation is known as "type II radio burst," and it is characterized by intense narrowband emissions and slow frequency drift (Wild and McCready, 1950; Reiner and Kaiser, 1999; Kong et al., 2014).

IP shocks are disturbances within the solar wind. If the CME is sufficiently strong and propagates toward Earth, the associated IP shock would reach Earth. Therefore, IP shocks are one of the manifestations of solar disturbances in IP spaces because their arrival at Earth's orbit corresponds to the sudden commencement of geomagnetic storms, marking the onset of corresponding geomagnetic disturbances (Gopalswamy et al., 2008b). Type II radio bursts provide information on the physical characteristics of IP shocks and their behavior because they traverse the solar corona and IP spaces. The IP shocks observed at 1 AU are associated with CME originating from the sun. They propagate into IP spaces at speeds ranging from hundreds to thousands of kilometers per second. When interacting with Earth's magnetic field, they can cause severe space weather effects and geomagnetic storms (Burlaga et al., 1981; Zhang and Burlaga, 1988; Gosling, 1993; Gonzalez et al., 1994; Schwenn et al., 2005).

The geoeffectiveness of CMEs is crucial in space weather research and forecasting, determining their ability to reach Earth, their arrival time, and their potential impact on Earth. The CME associated with type II radio bursts has greater energy than an ordinary CME (Gopalswamy et al., 2001). Furthermore, type II radio bursts are considered as direct indicators of CME-driven IP shocks (Lara et al., 2003; Gopalswamy et al., 2005; Vasanth et al., 2011). The frequency drift rate of type II radio bursts can be employed to estimate the velocity of CME-driven IP shocks. The occurrence frequency of type II radio bursts can be employed to estimate the height of the solar corona where the CME-driven shock originates. Type II radio bursts exhibit split-band structures that estimate the strength of coronal and IP magnetic fields; thus, it cannot be replaced by other methods. Studies reveal that CMEs associated with decametric type II radio bursts are faster, wider, and have higher energy levels (Gopalswamy et al., 2001; Lara et al., 2003). Therefore, researchers can utilize the characteristics of radio bursts near the sun and in IP spaces to predict the geoeffectiveness of the CMEs/shocks associated with IP type II bursts that are far from the sun (Gopalswamy et al., 2008b). For example (Valach et al., 2014), utilized decimetric type II radio bursts as inputs for their artificial neural network prediction method to forecast strong geomagnetic storms (Kumari et al., 2023). conducted a statistical analysis of type II bursts between 25 and 200 MHz during solar cycles 23 and 24, establishing a temporal correlation between these radio bursts and CME events.

This study investigated the causal relationship between IP radio bursts and the corresponding geomagnetic responses in Earth's space environment. We utilized existing observational datasets to compile and organize IP shock events detected by satellite instruments during solar cycles 23 and 24 (1996–2009). Additionally, we used lists of CME/IP coronal mass ejection (ICME) and type II IP radio burst events during the same period, forming a comprehensive dataset of solar-IP disturbance events. The remainder of this paper is organized as follows. Section 2 introduces the dataset used for the statistical analysis and method of event selection. Section 3 presents the statistical results regarding the correlations between the CME, type II radio bursts, and IP shocks. Section 4 discusses and summarizes the findings of statistical analyses.

2 Data and events

2.1 Event list

The data sources used in this study are as follows:

1. SOHO/LASCO records CME events in the catalog. https://cdaw.gsfc.nasa.gov/CME_list/

The coronal mass ejection information was obtained using the LASCO CME catalog maintained by the CDAW Data Center (Yashiro et al., 2004). The LASCO onboard the SOHO spacecraft provided the start time and linear initial velocity of CMEs. LASCO observations were employed to determine the CME height and its propagation in IP space. For each event, the catalog provided the appearance time of the CME in the LASCO C2 field of view (FOV), central position angle (CPA), angular width, height-time plots from linear and second-order fits, CME velocity, and other relevant information. The directory contained all CME manually identified from SOHO's LASCO since 1996. Additionally, it included kinematic characteristics, such as the start and end times, projected velocity, angular width, and mass, and the corresponding links for image and video downloads.

2. List of type II and Type IV Radio Burst Events Recorded by WIND/WAVES. https://spdf.gsfc.nasa.gov/pub/data/stereo/documents/websites/solar-radio/wind/data_products.html.

The catalog provided the start and stop times of II and types IV radio bursts and the upper and lower frequency limits. Most entries also included annotations and dynamic spectra of partial radio emissions.

3. The list of type II radio bursts recorded by Wind/WAVES along with associated flares and CME events. https://cdaw.gsfc.nasa.gov/CME_list/radio/waves_type2.html.

The radio burst catalog compiled in (Gopalswamy et al., 2019) includes information on type II radio bursts recorded by Wind/WAVES and their characteristics. However, this also contains information on associated CME, flares, the source region on the solar disk, and solar energetic particle (SEP) events. The provision of images and spectra for each type II IP radio burst and its related phenomena is also a crucial feature of this catalog. However, this enables users to correlate various events and utilize the tools provided for further online measurements, facilitating further research into potential solar bursts.

4. The list of IP shock events recorded by WIND. https://lweb.cfa.harvard.edu/shocks/wi_data/index.html.

Stevens and Kasper maintained the online database of IP shocks observed by the Wind and ACE spacecraft, which provide

information, such as the start and end times of the shock, and type of shock (Wu and Lepping, 2016; Wilson III et al., 2017).

5. The geomagnetic activity Dst index. https://wdc.kugi.kyoto-u.ac.jp/dst_final/index.html.

The Dst index was provided hourly by the Graduate School of Science and the Kyoto University Center for Planetary Magnetic and Space Physics Data Analysis. Additionally, it was employed to identify the presence of geomagnetic storms and determine their intensity levels of geomagnetic storms. The intensity of the geomagnetic storms was classified based on the Dst index. ICMEs that the reach Earth can impact its magnetosphere. The southward magnetic field within the CME can reconnect with Earth's magnetosphere, leading to responses, such as geomagnetic storms in Earth's space environment. The Dst index was employed to quantify the severity of the geomagnetic disturbances corresponding to the arrival of IP shocks on Earth.

6. List of ICME Events. https://izw1.caltech.edu/ACE/ASC/DATA/level3/icmetable2.htm.

IP shocks were driven by ICMEs. Based on their velocity and IP characteristics, the ICMEs may reach Earth within 1–5 days after the burst (Lawrance et al., 2016). The ICME list edited by Richardson and Cane(Cane and Richardson, 2003; Richardson and Cane, 2010) provided information on the timing and characteristics of solar-terrestrial disturbances, including CMEs, disturbances (related to the onset of geomagnetic storms and associated with shock arrival), ICMEs, and Dst index (Yashiro et al., 2004; Gopalswamy et al., 2009).

2.2 Event selection

Events from January 1996 to December 2019 were selected based on these websites, covering solar Cycles 23 and 24. After filtering and comparing these database directories, we collated and completed the relevant information for each event. Our statistical results show that 638 type II IP radio burst events and 541 IP shock events at the L1 point were identified (as illustrated in Table 1). In this study, "shock" events refer to shock events at the L1 point without a corresponding type II burst and CME. However, some of them may have corresponding geomagnetic responses. "Type II burst" events refers to cases with only type II radio burst events occurring without corresponding CME and shock events or where type II radio burst and CME events correspond one-to-one, without corresponding IP shock events. "Type II burst-shock" events refers to the type II bursts associated with the shocks reaching Earth, indicating type II burst events effective on Earth. These events are identified based on the following criteria: a frequency drift lasting from several hours to 4–5 days from the beginning of the type II. When the frequency decreases to approximately 30 kHz, the wind spacecraft can detect the density and velocity changes associated with the shock *in situ*. Based on the above-mentioned criteria, we identified 180 type II burst-shock events, as illustrated in Table 1. Additionally, we listed the occurrence time and type of IP shock. The date and time of first appearance in the LASCO/C2 FOV and the CPA, sky-plane width of CMEs, and each CME has three speeds: 1) linear speed obtained by fitting height-time measurements with a 1st order polynomial fit; 2) quadratic speed obtained by fitting height-time measurements with a 2nd order polynomial fit and evaluating the speed at the last (possible) height measurement; 3) the speed evaluated when the CME is at a height of 20 solar radii, similar to (2). Each CME is also characterized by an acceleration, mass and a kinetic energy. The end time, frequency, and frequency spectrum of type II burst. The Dst index, and peak time of Dst index. The start and end time, average speed, maximum speed, and transient speed of the ICME; and time of sudden onset of the associated geomagnetic storm. However, if a significant peak in the Dst index within 20–100 h after a CME occurs, it is associated with geomagnetic storms. Geomagnetic storms were classified into five categories based on the minimum value of the geomagnetic Dst index: weak (−30 to −50 nT), moderate (−50 to −100 nT), strong (−100 to −200 nT), severe (−200 to −350 nT), and great (<−350 nT). However, if Dst≤-50nT, this event was considered geoeffective (Loewe and Prölss, 1997; Gopalswamy et al., 2007). Figure 1 shows an example of a CME event associated with an intense geomagnetic storm and an IP type II burst.

TABLE 1 Statistical analysis of geoeffective events during solar cycles 23 and 24.

Events	Solar cycle		
	23	24	23 + 24
Type II bursts	404	234	638
Shocks	351	190	541
"Type II burst-shock" events	143	37	180

3 Statistical results

This section presents the statistical results of the correlations among CMEs, type II radio bursts, and IP shocks. Subsequently, it discusses the statistical analysis of geoeffective events associated with type II radio bursts.

3.1 Arrival probability of type II burst-shock events

Figure 2 shows the monthly distribution of sunspots from 1996 to 2019 (solar cycles 23 and 24). Solar cycle 23 spanned from the end of 1996 to the end of 2008. However, solar cycle 24 decreased in sunspot numbers compared with solar cycle 23. Figure 3 shows the distribution of type II radio bursts recorded by Wind/WAVES during these two cycles, whereby the orange bars represent the total number of type II radio bursts per year. The green bars indicate the number of type II bursts associated with shocks that reached Earth. Overall, the distribution of type II bursts correlated with sunspot numbers, with fewer events occurring during the solar minima and more events occurring during the solar maxima. However, in 1999 and 2005, the occurrence rates of CMEs were anomalous, leading to a significant decrease in event count.During solar cycles 23 and 24,

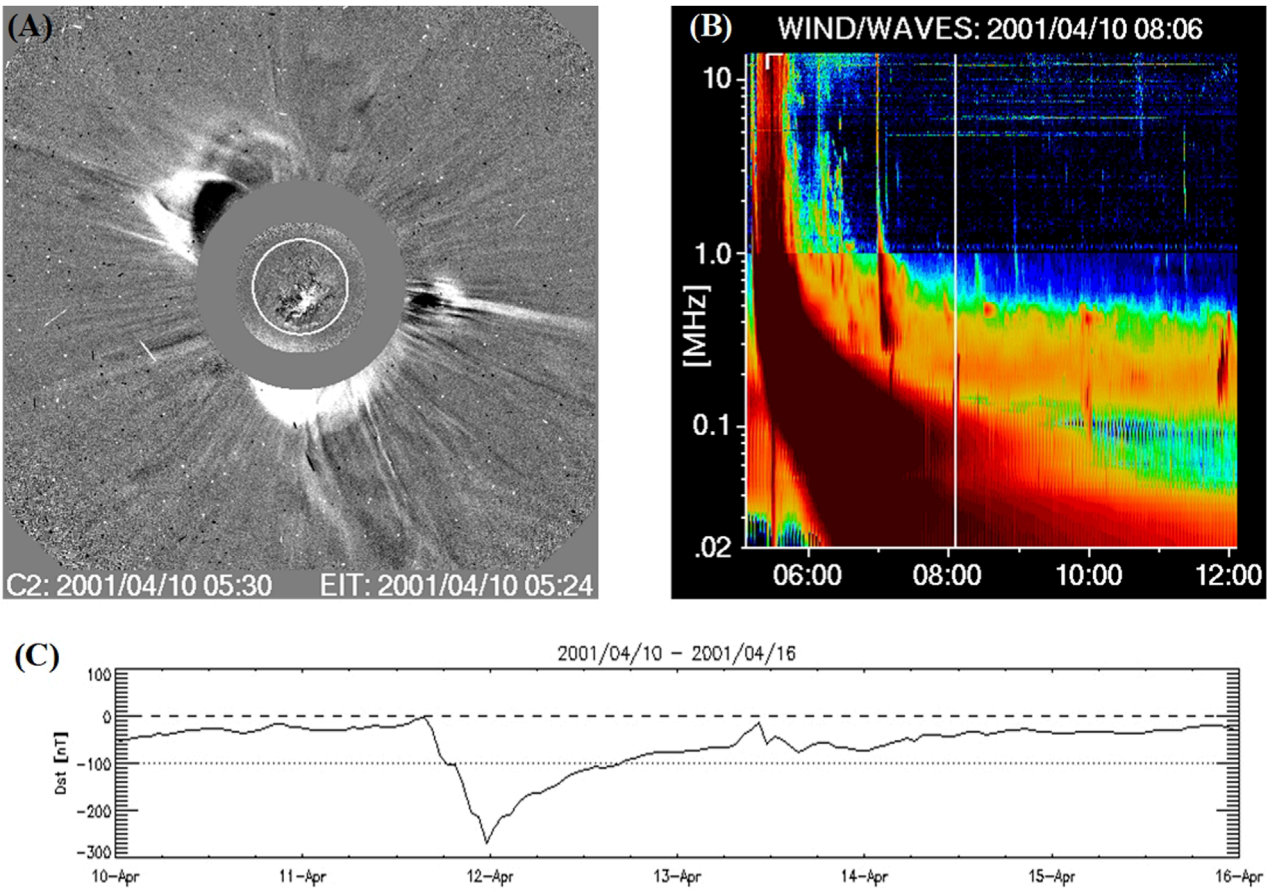

FIGURE 1
Example of CME-type II burst events associated with a major geomagnetic storm. **(A)** LASCO C2 running difference image of the CME. **(B)** Corresponding dynamic radio spectrum of the IP type II burst recorded by Wind/WAVES. **(C)** Relevant Dst profile from the Kyoto geomagnetic database.

Wind/WAVES recorded 638 type II bursts, while 541 shocks were observable at the L1 point by the wind. Additionally, 180 type II burst-shock events occurred, as illustrated in Table 1. Approximately 28.21% (type II burst-shock/type II bursts) of the type II burst-associated shocks propagated to Earth. Approximately 33.27% (type II burst-shock/shocks) of the IP shocks on Earth were associated with type II bursts.

3.2 Cutoff frequency of type II radio bursts and their associated shock's arrival probability

The study aimed to investigate if the cutoff frequency of type II bursts can effectively predict the geo-effectiveness of the CME/shock. Among the "type II burst-shock" events, 19.49% were associated with "type II burst-shock" events with cutoff frequencies of approximately 1 MHz, 29.29% with "type II burst-shock" events with cutoff frequencies of approximately 100 kHz, and 50.96% with "type II burst-shock" events with cutoff frequencies of approximately 10 kHz. Figure 4 shows a histogram of the probability of "type II burst-shock" events reaching Earth for various cutoff frequencies from 1996 to 2019. The x-axis represents the cutoff frequencies of type II bursts, ranging from 10 kHz to 10^4 kHz. The y-axis represents the corresponding probability of reaching Earth. We conducted a regression analysis on the distribution of the histograms, which shows an exponentially decreasing trend, indicating that the corresponding shocks of the type II bursts with lower cutoff frequencies can potentially reach the Earth. The adjusted R square of the fitted equation of the regression curve is 0.9877, which indicates the statistical significance of the fitted result, thus confirming the reliability of the empirical relationship of the fitted curve. Therefore, the presence of type II bursts and their corresponding cutoff frequencies can serve as indicators for the corresponding shock's arrival on Earth. Lower cutoff frequencies of type II bursts increase the IP shock reaching Earth.

3.3 Distribution of cutoff frequencies of type II radio bursts and the related geomagnetic storm intensity

Because of the rarity of great storms (Dst < −350 nT) occurring between 1996 and 2009, this study categorized geomagnetic storm events into four classes: weak (−30 to −50 nT), moderate (−50 to

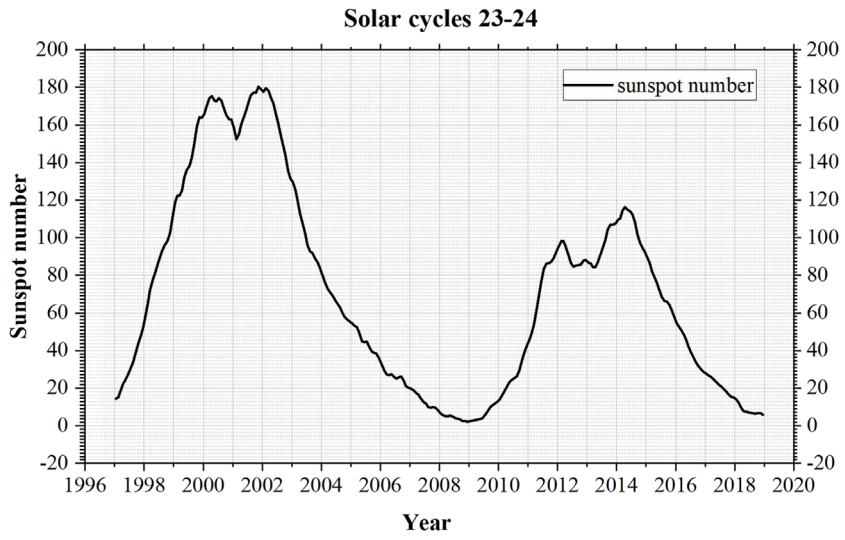

FIGURE 2
Monthly distribution of sunspot numbers from 1996 to 2019 (solar cycles 23 and 24).

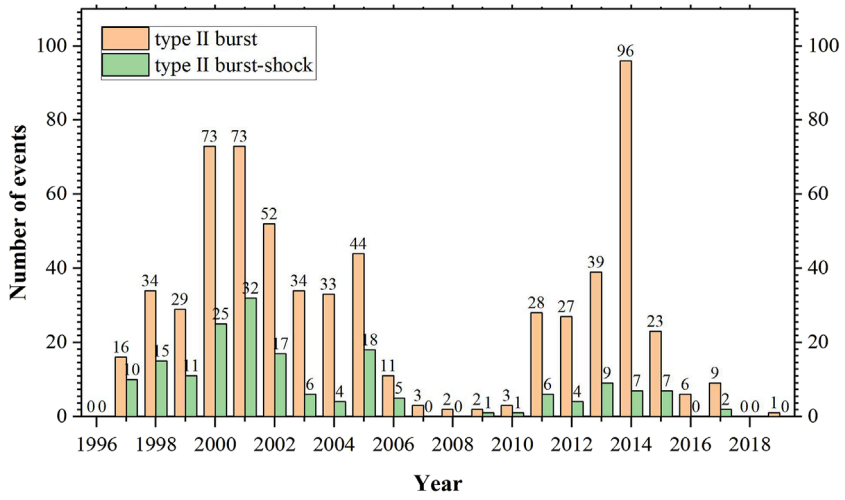

FIGURE 3
The annual distribution of type II bursts (orange) and "type II burst-shock" events (green) for solar cycles 23 and 24 (1996–2019).

−100 nT), strong (−100 to −200 nT), severe, and great (<−200 nT). During solar cycles 23 and 24, 426 geomagnetic storms occurred. Approximately 23% of which were associated with type II burst-shock events (99 events).

To demonstrate the impact of type II burst cutoff frequencies on the occurrence and intensity of geomagnetic storms and reveal whether the cutoff frequency of these bursts can serve as an effective indicator for geomagnetic storm forecasting, we computed the number of events associated with type II bursts at various cutoff frequencies. Figure 5 shows the distribution of geomagnetic response events (average Dst index) for each type of shock event. This indicates that the lower the cutoff frequency of a type II burst, the stronger the geomagnetic response of the corresponding shock; additionally, type II burst-shock events have a stronger geomagnetic response than shock events without a corresponding type II burst. This implies that the presence of IP type II radio bursts and their corresponding cutoff frequencies can be used as a measure of the geomagnetic effect of CMEs or shocks on Earth.

4 Discussion

This study investigated the geoeffectiveness of solar-IP disturbances associated with type II bursts and IP shocks during solar cycles 23 and 24 (1996–2009). The results showed that approximately 28.21% of the type II radio bursts were associated with IP shocks on Earth, whereas 33.27% of the IP shock events

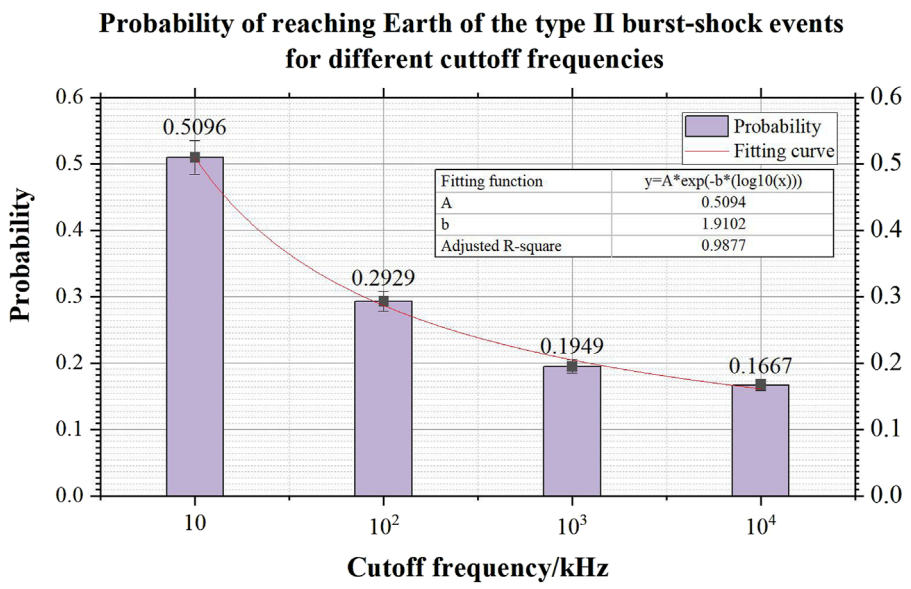

FIGURE 4
Probability of reaching Earth of the type II burst-shock events for different cuttoff frequencies.

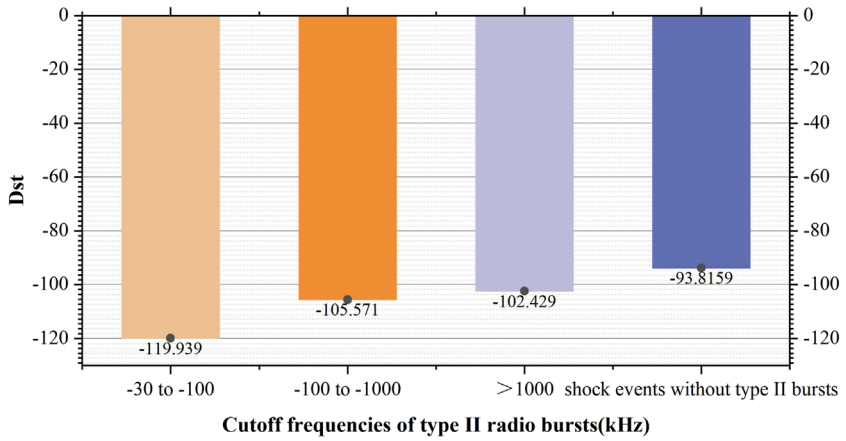

FIGURE 5
Bar chart illustrating the averaged geomagnetic storm intensity caused by the type II radio bursts with different cutoff frequencies.

on Earth were associated with type II radio bursts. Regarding the impact of the cutoff frequency of type II radio bursts on the intensity of the geomagnetic response induced by the corresponding CME/shock, IP type II radio bursts and their cutoff frequencies can serve as indicators of the geoeffectiveness of CME/shock on Earth. IP shocks accompanying type II bursts induce a stronger geomagnetic response than shocks not associated with type II bursts. Lower cutoff frequencies of Type II bursts typically indicate that the associated shocks are more energetic and propagating at higher speeds. This increase in energy and velocity can result in stronger emissions in the radio spectrum. As these intensified shocks travel through the solar atmosphere and expand outward, they have a greater likelihood of reaching Earth. Therefore, lower cutoff frequencies of the type II radio bursts increase the probability of the corresponding shock's reaching Earth, intensifying the geomagnetic response induced by the shocks, the presence of IP type II radio bursts can serve as indicators for predicting the geoeffectiveness of the corresponding IP shocks on Earth. In the future, this research will be expanded to integrate with predictive models of shock arrival time and imaging observations of type II bursts. Leveraging the established white light imaging observation techniques, multiple datasets can be merged to enhance the understanding of the kinematic process and origin of these type II radio bursts. This approach is beneficial for increasing the accuracy of predicting severe space weather impacts associated with solar and interplanetary disturbances.

Data availability statement

The original contributions presented in the study are included in the article/supplementary material, further inquiries can be directed to the corresponding author.

Author contributions

JY: Formal Analysis, Funding acquisition, Methodology, Supervision, Validation, Writing–review and editing. QY: Data curation, Investigation, Validation, Visualization, Writing–original draft.

Funding

The author(s) declare that no financial support was received for the research, authorship, and/or publication of this article.

Acknowledgments

The authors are grateful to everyone who contributed to this topic through their discussions and collaborations. This CME catalog was generated and maintained at the CDAW Data Center by NASA and the Catholic University of America in cooperation with the Naval Research Laboratory. SOHO is a project of international cooperation between ESA and NASA. We also acknowledge the online database of IP shocks observed by the Wind and ACE spacecraft. We also acknowledge the website https://spdf.gsfc.nasa.gov/pub/data/stereo/documents/websites/solar-radio/wind/data_products.html for providing the catalog of type II bursts and their associated CMEs. We thank the geomagnetic observatories [Kakioka (JMA), Honolulu and San Juan (USGS), Hermanus (RSA), INTERMAGNET, and many others] for their cooperation in making the final Dst index available.

Conflict of interest

The authors declare that the research was conducted in the absence of any commercial or financial relationships that could be construed as a potential conflict of interest.

Publisher's note

References

Burlaga, L., Sittler, E., Mariani, F., and Schwenn, a. R. (1981). Magnetic loop behind an interplanetary shock: voyager, helios, and imp 8 observations. *J. Geophys. Res. Space Phys.* 86, 6673–6684. doi:10.1029/ja086ia08p06673

Cane, H., and Richardson, I. (2003). Interplanetary coronal mass ejections in the near-earth solar wind during 1996–2002. *J. Geophys. Res. Space Phys.* 108. doi:10.1029/2002ja009817

Gonzalez, W., Joselyn, J.-A., Kamide, Y., Kroehl, H. W., Rostoker, G., Tsurutani, B. T., et al. (1994). What is a geomagnetic storm? *J. Geophys. Res. Space Phys.* 99, 5771–5792. doi:10.1029/93ja02867

Gopalswamy, N., Aguilar-Rodriguez, E., Yashiro, S., Nunes, S., Kaiser, M., and Howard, R. (2005). Type ii radio bursts and energetic solar eruptions. *J. Geophys. Res. Space Phys.* 110. doi:10.1029/2005ja011158

Gopalswamy, N., Akiyama, S., and Yashiro, S. (2008a). Major solar flares without coronal mass ejections. *Proc. Int. Astronomical Union* 4, 283–286. doi:10.1017/s174392130902941x

Gopalswamy, N., Mäkelä, P., and Yashiro, S. (2019). *A catalog of type ii radio bursts observed by wind/waves and their statistical properties*. arXiv preprint arXiv:1912.07370.

Gopalswamy, N., Yashiro, S., and Akiyama, S. (2007). Geoeffectiveness of halo coronal mass ejections. *J. Geophys. Res. Space Phys.* 112. doi:10.1029/2006ja012149

Gopalswamy, N., Yashiro, S., Kaiser, M., Howard, R., and Bougeret, J.-L. (2001). Characteristics of coronal mass ejections associated with long-wavelength type ii radio bursts. *J. Geophys. Res. Space Phys.* 106, 29219–29229. doi:10.1029/2001ja000234

Gopalswamy, N., Yashiro, S., Michalek, G., Stenborg, G., Vourlidas, A., Freeland, S., et al. (2009). The soho/lasco cme catalog. *Earth, Moon, Planets* 104, 295–313. doi:10.1007/s11038-008-9282-7

Gopalswamy, N., Yashiro, S., Xie, H., Akiyama, S., Aguilar-Rodriguez, E., Kaiser, M. L., et al. (2008b). Radio-quiet fast and wide coronal mass ejections. *Astrophysical J.* 674, 560–569. doi:10.1086/524765

Gosling, J. T. (1993). The solar flare myth. *J. Geophys. Res. Space Phys.* 98, 18937–18949. doi:10.1029/93ja01896

Hundhausen, A. (1987). The origin and propagation of coronal mass ejections (r). *Sixth Int. Sol. wind Conf.* 2, 181.

Kong, X., Chen, Y., Guo, F., Feng, S., Wang, B., Du, G., et al. (2014). The possible role of coronal streamers as magnetically closed structures in shock-induced energetic electrons and metric type ii radio bursts. *Astrophysical J.* 798, 81. doi:10.1088/0004-637x/798/2/81

Kumari, A., Morosan, D. E., Kilpua, E., and Daei, F. (2023). Type ii radio bursts and their association with coronal mass ejections in solar cycles 23 and 24. *Astronomy and Astrophysics* 675, A102. doi:10.1051/0004-6361/202244015

Lara, A., Gopalswamy, N., Nunes, S., Munoz, G., and Yashiro, S. (2003). A statistical study of cmes associated with metric type ii bursts. *Geophys. Res. Lett.* 30. doi:10.1029/2002gl016481

Lawrance, M. B., Shanmugaraju, A., Moon, Y.-J., Ibrahim, M. S., and Umapathy, S. (2016). Relationships between interplanetary coronal mass ejection characteristics and geoeffectiveness in the rising phase of solar cycles 23 and 24. *Sol. Phys.* 291, 1547–1560. doi:10.1007/s11207-016-0911-4

Loewe, C., and Prölss, G. (1997). Classification and mean behavior of magnetic storms. *J. Geophys. Res. Space Phys.* 102, 14209–14213. doi:10.1029/96ja04020

Reiner, M., and Kaiser, M. (1999). High-frequency type ii radio emissions associated with shocks driven by coronal mass ejections. *J. Geophys. Res. Space Phys.* 104, 16979–16991. doi:10.1029/1999ja900143

Richardson, I. G., and Cane, H. V. (2010). Near-earth interplanetary coronal mass ejections during solar cycle 23 (1996–2009): catalog and summary of properties. *Sol. Phys.* 264, 189–237. doi:10.1007/s11207-010-9568-6

Schwenn, R., Dal Lago, A., Huttunen, E., and Gonzalez, W. D. (2005). The association of coronal mass ejections with their effects near the earth. *Ann. Geophys.* 23, 1033–1059. doi:10.5194/angeo-23-1033-2005

Valach, F., Bochníček, J., Hejda, P., and Revallo, M. (2014). Strong geomagnetic activity forecast by neural networks under dominant southern orientation of the interplanetary magnetic field. *Adv. Space Res.* 53, 589–598. doi:10.1016/j.asr.2013.12.005

Vasanth, V., Umapathy, S., Vršnak, B., and Anna Lakshmi, M. (2011). Characteristics of type-ii radio bursts associated with flares and cmes. *Sol. Phys.* 273, 143–162. doi:10.1007/s11207-011-9854-y

Wild, J., and McCready, L. (1950). Observatioas of the spectrum of high-intensity solar radiation at metre wavelengths. i. the apparatus and spectral types of solar burst observed. *Aust. J. Chem.* 3, 387–398. doi:10.1071/ch9500387

Wilson III, L., Koval, A., Szabo, A., Stevens, M., Kasper, J., Cattell, C., et al. (2017). Revisiting the structure of low-mach number, low-beta, quasi-perpendicular shocks. *J. Geophys. Res. Space Phys.* 122, 9115–9133. doi:10.1002/2017ja024352

Wu, C.-C., and Lepping, R. P. (2016). Relationships among geomagnetic storms, interplanetary shocks, magnetic clouds, and sunspot number during 1995–2012. *Sol. Phys.* 291, 265–284. doi:10.1007/s11207-015-0806-9

Yashiro, S., Gopalswamy, N., Michalek, G., St. Cyr, O., Plunkett, S., Rich, N., et al. (2004). A catalog of white light coronal mass ejections observed by the soho spacecraft. *J. Geophys. Res. Space Phys.* 109. doi:10.1029/2003ja010282

Zhang, G., and Burlaga, L. (1988). Magnetic clouds, geomagnetic disturbances, and cosmic ray decreases. *J. Geophys. Res. Space Phys.* 93, 2511–2518. doi:10.1029/ja093ia04p02511